



**HAL**  
open science

## Polymorphic Dynamics of Microtubules

Hervé Mohrbach, Albert Johner, Igor M. Kulic

► **To cite this version:**

Hervé Mohrbach, Albert Johner, Igor M. Kulic. Polymorphic Dynamics of Microtubules. 2010. hal-00509368

**HAL Id: hal-00509368**

**<https://hal.science/hal-00509368>**

Preprint submitted on 12 Aug 2010

**HAL** is a multi-disciplinary open access archive for the deposit and dissemination of scientific research documents, whether they are published or not. The documents may come from teaching and research institutions in France or abroad, or from public or private research centers.

L'archive ouverte pluridisciplinaire **HAL**, est destinée au dépôt et à la diffusion de documents scientifiques de niveau recherche, publiés ou non, émanant des établissements d'enseignement et de recherche français ou étrangers, des laboratoires publics ou privés.

# Polymorphic Dynamics of Microtubules

Hervé Mohrbach<sup>1</sup>, Albert Johner<sup>2</sup> and Igor M. Kulić<sup>2\*</sup>

<sup>1</sup>*Groupe BioPhysStat, Université Paul Verlaine, 57078 Metz, France*

<sup>2</sup>*CNRS, Institut Charles Sadron, 23 rue du Loess BP 84047, 67034 Strasbourg, France*

(Dated: May 7, 2010)

Starting from the hypothesis that the tubulin dimer is a conformationally bistable molecule - fluctuating between a curved and a straight configuration at room temperature - we develop a model for polymorphic dynamics of the microtubule lattice. We show that tubulin bistability consistently explains unusual dynamic fluctuations, the apparent length-stiffness relation of grafted microtubules and the curved-helical appearance of microtubules in general. Analyzing experimental data we conclude that taxol stabilized microtubules exist in highly cooperative yet strongly fluctuating helical states. When clamped by the end the microtubule undergoes an unusual zero energy motion - in its effect reminiscent of a limited rotational hinge.

PACS numbers: 87.16.Ka, 82.35.Pq, 87.15.-v

Microtubules are the stiffest cytoskeletal component and play versatile and indispensable roles in living cells. They act as cellular bones, transport roads [1] and cytoplasmic stirring rods [2]. Microtubules consist of elementary building blocks - the tubulin dimers - that polymerize head to tail into linear protofilaments (PFs). PFs themselves associate side by side to form the hollow tube structure known as the microtubule (MT). Despite a long history of their biophysical study a deeper understanding of MT's elastic and dynamic properties remains elusive to this date. Besides the unusual polymerization related non-equilibrium features like "treadmilling" and the dynamic instability there are a number of other experimental mysteries - in thermal equilibrium - that presently defy coherent explanations, most notably: (i) The presence of high "intrinsic curvature" [3]-[6] of unclear origin, also identified as a long wave-length helicity [3]. (ii) In various active bending [7] or thermal fluctuation experiments [4][5][8] MTs display length dependent, even non-monotonic apparent stiffness [5]. (iii) They exhibit unusually slow thermal dynamics in comparison with standard semiflexible filaments [5][6].

The most bizarre and controversial feature (ii) has been the subject of much debate and some theoretical explanation attempts based on low shear stiffness modulus have been put forward [9]. However a careful reanalysis of clamped MT experiments, Figs 2, 3 reveals two features not captured by these initial models: the lateral end-fluctuations scale as  $\sim L^2$  while the relaxation times scale as  $\sim L^3$ . This exotic behavior naively suggests the presence of a limited angular hinge at the MT clamping point. On the other hand artifacts that could trivially lead to a "hinged behavior" (like loose MT attachment and punctual MT damage) were specifically excluded in experiments [4][5]. We will outline here a model based on *internal* MT dynamics explaining phenomena (i)-(iii). It leads us to the origin of MT helicity (i) implying (ii)-(iii) as most natural corollaries [10]. The two central assumptions of our model are as follows: (I) The tubulin

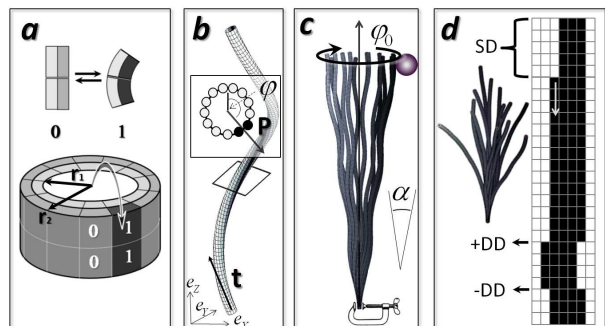


FIG. 1: Polymorphic Tube Model: (a) The tubulin dimer fluctuates between two states  $\sigma = 0, 1$  (straight / curved), (b) Tubulin switching on one MT side leads to spontaneous breaking of symmetry. Combined with the built-in lattice twist MT forms a polymorphic helix. The polymorphic order parameter  $P$  with phase angle  $\phi$  describes the distribution of tubulin states in the cross section. (c) Polymorphic wobbling - the zero-energy motion of the phase angle  $\alpha$  at each cross-section. It is responsible for the rotation on a cone with opening angle  $\alpha$  when clamped by the end. (d) Defects in polymorphic order: Single defects (SD) have a cost proportional to their length. Double defects (DD) give only local energy contribution.

dimer is a conformationally multistable entity and fluctuates between at least 2 states on experimental time scales. (II) There is a nearest-neighbor cooperative interaction of tubulin states along the PF axis. We are lead to assumptions I-II from several independent directions: *First*, the experimentally observed MT helicity [3] implies that there is a symmetry breaking mechanism of individual PF's conformational properties. In analogy to the classic case of bacterial flagellum the existence of helices in azimuthally symmetric bundles also necessitates a cooperative longitudinal interaction along protofilaments [11][12]. *Second*, investigations of single protofilament conformations by Elie-Caille et al [13] reveal that a single taxol- PF can coexist in at least 2 states with comparable free energy: a straight state  $\kappa_{PF} \approx 0$  and a weakly curved

state with intrinsic curvature  $\kappa_{PF} \approx 1/250nm$ . These authors also point out the apparent cooperative nature of straight to curved transition within single PFs. *Third*, when mechanically buckled by AFM tips tubulin dimers occasionally switch back to the initial straight conformation [14]. *Fourth*, tubulin multistability was inferred from the formation of stable circular MT arcs in kinesin driven gliding assays by Amos & Amos [15]. Unfortunately their clear, seminal observations were subsequently forgotten for decades leading to much of the confusion about MTs we are witnessing today.

*Polymorphic MT Model.* Starting from assumptions I – II we model the tubulin dimer state by a two state variable  $\sigma_n(s) = 0,1$  (the tubulin dimer in the "straight"/"curved" state, cf. Fig. 1a) at each lattice site with circumferential PF index  $n = 1, \dots, N$  ( $N = 11 - 16$  number of PFs) at longitudinal arclength centerline position  $s$ . The total elastic + conformational energy can be written as  $E_{MT} = \int_0^L (e_{el} + e_{trans} + e_{inter}) ds$  with

$$e_{el} = \frac{Y}{2} \int \int (\varepsilon - \varepsilon_{pol})^2 r dr d\alpha \quad (1)$$

$$e_{trans} = -\frac{\Delta G}{b} \sum_{n=1}^N \sigma_n(s), \quad (2)$$

$$e_{inter} = -\frac{J}{b} \sum_{n=1}^N (2\sigma_n(s) - 1)(2\sigma_n(s+b) - 1) \quad (3)$$

where the integration in  $e_{el}$  goes over the annular MT cross-section with  $r_1 \approx 7.5nm$ ,  $r_2 \approx 11.5nm$  the inner and outer MT radii, with  $\Delta G > 0$  the energy difference between the 0 and 1 state and  $b \approx 8nm$  the monomer length,  $J$  the "Ising" cooperative coupling term along the PF contour and with the polymorphism induced pre-strain  $\varepsilon_{pol} \propto \varepsilon_{PF} \sigma_n(s)$  [16] where  $\varepsilon_{PF}$  is the strain generated in the curved state. The latter can be estimated from the switched PF curvature  $\kappa_{PF} \approx (250nm)^{-1}$  [13] to be  $\varepsilon_{PF} = d_{PF} \kappa_{PF} / 2 \approx 10^{-2}$ . For an isotropic Euler-Kirchhoff beam, the actual material deformations are related to the centerline curvature via  $\varepsilon = -\vec{\kappa} \cdot \vec{r}$  with  $\vec{r}$  the radial vector in the cross-section.

Upon inspection it becomes clear that the phase behavior (straight or curved state stability) is contained in the interplay of the first two terms  $e_{el}$  and  $e_{trans}$  while the thermal dynamics is governed by the 3rd  $e_{inter}$  which rules over defect behavior (cf. Fig. 1d). To understand the basic behavior we first consider a short MT section along which the PFs are in a uniform state  $\sigma_n(s) = \sigma_n(s+b)$  ( $e_{inter} = \text{const.}$  can be dropped). Furthermore we resort to the single block ansatz, i.e. at each cross-section there is only one continuous block of switched PFs of length  $p$ . This ansatz was successfully used by Calladine in modelling bacterial flagellin polymorphic states [11]. In this approximation the energy density becomes

$$e = \frac{B}{2} \left( (\kappa - \kappa_{pol}(p))^2 + \kappa_1^2 \left( \gamma \frac{\pi}{N} p - \sin^2 \left( \frac{\pi}{N} p \right) \right) \right) \quad (4)$$

with the bending modulus  $B = \frac{Y\pi}{4} (r_2^4 - r_1^4)$  and the polymorphic curvature  $\kappa_{pol}(p) = \kappa_1 \sin \left( \frac{\pi}{N} p \right)$  with  $\kappa_1 = \frac{\kappa_{PF}(r_2 - r_1)^2}{\pi(r_1^2 + r_2^2)}$ . The MT phase behavior depends on the polymorphic-elastic competition parameter  $\gamma = \frac{\kappa_{PF}}{\kappa_1} - \frac{2N\Delta G}{bB\kappa_1^2}$ . Physically,  $\gamma$  measures the ratio between polymorphic energy of tubulin switching and the elastic cost of the transition. For  $\gamma < -1$  all the PFs are in the (highly prestrained) state  $\sigma = 1$  while for  $\gamma > 1$  all them are in the state  $\sigma = 0$  - both corresponding to a straight MT. For  $-1 < \gamma < 1$  we have coexistence of 2 locally (meta) stable states : straight ( $p = 0$  or  $p = N$ ) and curved state with  $p > 0$ . For  $-\bar{\gamma} < \gamma < \bar{\gamma}$  with  $\bar{\gamma} \approx 0.72$  the curved state is the absolute energy minimum and the straight state is only metastable. Therefore in this regime, the ground state of a microtubule bearing natural lattice twist will be helical (cf. Fig. 1b). Assuming a stable helical state as observed in [3] we have  $p/N \in [1/4, 1/2]$  giving us an estimate for the radius of curvature  $\kappa_{pol}^{-1} \approx 9 - 14\mu m$ . This compares favorably with an estimate of observed helices  $\kappa^{-1} \approx 11\mu m$  from [3]. The helical stability and the magnitude of the protofilament curvature  $\kappa_{PF} \approx 1/250nm$  [13] with a typical protein Young modulus  $Y \approx 1-10GPa$ , allows us also a simple estimate of the transition energy per monomer  $\Delta G \approx +1.1$  to  $+11kT$ . In general, the energy in Eqs.1-3 gives rise to a complex behavior and we focus on basic phenomena. It turns out that a most remarkable deviation from standard wormlike chain behavior comes from the change of polymorphic phase that we consider in the following.

*Polymorphic Phase Dynamics.* To better understand the central phenomenon, we define at each MT cross-section the complex *polymorphic order parameter*  $P(s) = \sum_{n=1}^N e^{2\pi i n/N} \sigma_n(s) = |P(s)| e^{i\phi(s)}$  where  $|P(s)|$  denotes the "polymorphic modulus" and  $\phi$  the "polymorphic phase" (cf. Fig. 1b). The polymorphic state can then be described by the local (complex) centerline curvature  $\hat{\kappa}_{pol}(s) = \kappa_0 e^{iq_0 s} P(s)$  with  $\kappa_0 = \kappa_1 \sin \pi/N$  and  $q_0$  the natural lattice twist that varies with PF number [17]. This gives rise to a helical MT shape described by the curvature  $|\hat{\kappa}_{pol}| = \kappa_{pol}$  and torsion  $\tau \approx \phi' + q_0$ . For large acting forces both the polymorphic phase  $\phi$  and amplitude  $|P|$  will vary along the contour, however for small (thermal) perturbations the phase fluctuations will be dominant [18]. Based on this and on the observation of stable helical states [3] we will now assume  $|P| = \text{const.}$  and write the total energy of the MT whose centerline deflection is described by a complex angle  $\theta(s) = \theta_x(s) + i\theta_y(s)$  (deflection angles in x/y direction) as follows:

$$E_{tot} = E_{el}(\theta, \phi) + E_{pol}(\phi) \quad (5)$$

The first energy term is the "wormlike-chain" bending contribution  $E_{el}(\theta, \phi) = \frac{B}{2} \int |\theta' - \hat{\kappa}_{pol}|^2 ds$ . The second term is the polymorphic phase energy  $E_{pol}(\phi) =$

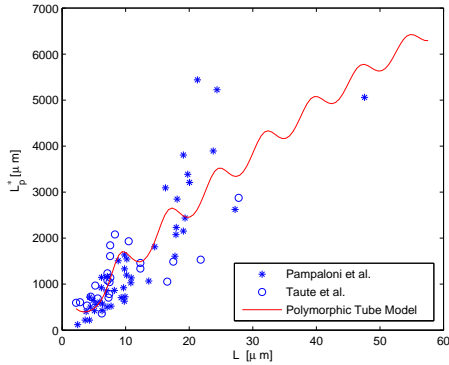


FIG. 2: Effective persistence length  $l_p^*(s)$  as a function of the position from the attachment point along the MT contour. The experimental and theoretical prediction with  $l_B = 25\text{mm}$ ,  $\lambda = 7.5\mu\text{m}$ ,  $\kappa_0^{-1} = 18\mu\text{m}$ ,  $q_0 l_\phi \gg 1$ .

$\frac{C_\phi}{2} \int_0^L \phi'^2 ds$  with the polymorphic phase stiffness  $C_\phi = k_B T \frac{N^2 b}{8\pi^2} (2 + e^{2J/k_B T})$  which can be related to the density of double defects with energy  $2J$  (cf. Fig. 1d), giving rise to a new length scale - the polymorphic phase coherence length  $l_\phi = C_\phi/k_B T$ .

The most unusual property of a polymorphic chain is reflected in the rotational invariance of  $E_{pol}(\phi)$ . The broken cylindrical to helical symmetry of the straight state is restored by the presence of a "Goldstone mode"  $\phi \rightarrow \phi + \phi_0$  [19] consisting of a rotation of  $P$  by an arbitrary angle  $\phi_0$  in the material frame (cf. Fig. 1c). This mode that we will call the "wobbling mode" is a fundamental property of a helically polymorphic filament. The wobbling mode leads to dramatic effects on chain's fluctuations and is the clue to the resolution of mysteries (i)-(iii). To see this we will first investigate the static properties resulting in length dependent variations of the persistence length.

*Persistence Length Anomalies.* Among several definitions of the persistence length [20] we consider for direct comparison with experiments [4][5], the lateral fluctuation persistence length  $l_p^*(s) = (2/3) s^3 / \langle |\rho(s)|^2 \rangle$  with  $\rho(s) = x(s) + iy(s)$  the transverse displacement at position  $s$  of a MT clamped at  $s = 0$  and  $\langle \dots \rangle$  the statistical average. It is easy to see from Eq. 5 that for small deflections,  $\rho$  decouples into independent elastic and polymorphic displacements  $\rho(s) = \rho_{el} + \rho_{pol}$ , such that  $l_p^* = (l_{pol}^{*-1} + l_B^{-1})^{-1}$  with  $l_{pol}^* = (2/3) s^3 / \langle |\rho_{pol}|^2 \rangle$  where  $\rho_{pol} = \kappa_0 \int_0^s \int_0^{s_1} e^{iq_0 \tilde{s} + i\phi(\tilde{s})} d\tilde{s} ds_1$ . The coherent helix nature of the MT observed in [3] and the absence of a plateau in  $l_p^*$  imply [21] that  $l_\phi \gg \lambda = 2\pi q_0^{-1}$  (the helix wave length). In that limit we obtain  $\langle |\rho_{pol}|^2 \rangle \approx \kappa_0^2 q_0^{-2} [\frac{2}{q_0^2} + s^2 + \frac{s^3}{3l_\phi} - \frac{2}{q_0^2} e^{-\frac{s}{2l_\phi}} ((1 + \frac{s}{2l_\phi}) \cos q_0 s + s q_0 \sin q_0 s)]$ . Whereas for an ideal WLC  $l_p^* = l_B \equiv B/k_B T$  is position and definition independent,

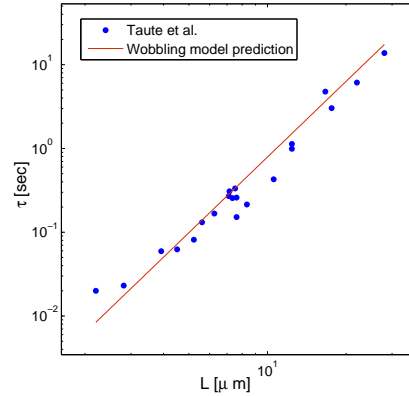


FIG. 3: Longest relaxation time of a microtubule of length  $L$ , experimental data from [5] and theoretical prediction from the wobbling mode approximation and the wobbling angle  $\alpha = 2\kappa_0/q_0 \approx 7.9^\circ$  extracted from static data [4][5], Fig. 2.

the polymorphic fluctuations induce a strong position / distance dependence - a behavior that could be interpreted as "length dependent persistence length". Indeed for  $l_\phi \gg s \gg q_0^{-1}$  the persistence length displays a non-monotonic oscillatory behavior around a nearly linearly growing average value  $l_p^*(s) \approx \frac{2}{3} \frac{q_0^2}{\kappa_0^2} s + \frac{4}{3} \frac{q_0}{\kappa_0^2} \sin(q_0 s)$ . This oscillation is related to the helical ground state while the linear growth  $l_p^*(s) \propto \alpha^2 s$  is associated to the conical rotation of the clamped chain (wobbling mode), cf. Fig. 1c, with an angle  $\alpha = 2\kappa_0 q_0^{-1}$ . For  $s \gg l_\phi$  the saturation regime with a renormalized  $l_p^*(\infty) = 1 / (l_{pol}^{-1} + l_B^{-1})$  with  $l_{pol} = 2l_\phi q_0^2 \kappa_0^{-2}$  is reached. The theory can now be compared with the experimental data [4][5] (cf. Fig. 2) that reveal several interesting characteristics in agreement with predictions. In particular the mean linear growth of  $l_p^*(L)$  (single parameter fit  $l_p^* \sim L^\delta$  gives  $\delta = 1.05$ ) and the non-monotonic  $l_p^*(L)$  dependence [5] are well captured by the theory. The linearly growing experimental spread of  $l_p^*$  with  $L$  is likely linked to the spread of  $q_0$  in the MT lattice populations [17]. The large length plateau  $s \gg l_\phi$  is not reached even for longest MTs ( $\sim 50\mu\text{m}$ ) in agreement with coherent helices [3]. Our best comparison between theory and experiments (cf. Fig. 2) gives  $l_B = 25\text{mm}$  corresponding to  $Y \approx 9\text{GPa}$  (proteins with  $Y$  up to  $19\text{GPa}$  exist [22]) and a helix wave length  $\lambda \approx 7.5\mu\text{m}$ . This is close to the expected  $6\mu\text{m}$  corresponding to the twist [17] of the predominant 14 PF MTs fraction in the in-vitro MTs preparation of [4][5]. It turns out that  $l_B$  is larger than in previous studies  $l_B \sim 1 - 6\text{mm}$  where however polymorphic fluctuations were neglected. The absence of the plateau also allows a lower estimate of the coherence length  $l_\phi > 55\mu\text{m}$  and the coupling constant  $J > 4k_B T$ .

*Polymorphic Phase Dynamics.* To describe the MT fluctuation dynamics we consider the total dissipa-

tion functional  $P_{diss} = P_{ext} + P_{int}$  which is composed of an internal dissipation contribution  $P_{int} = \frac{1}{2}\xi_{int} \int \dot{\phi}^2 ds$  and an external hydrodynamic dissipation  $P_{ext} = \frac{1}{2}\xi_{\perp} \int |\dot{\rho}|^2 ds$  with  $\xi_{\perp} = 4\pi\eta/(\ln(2L/r) - 1/2)$  the lateral friction constant,  $\eta$  the solvent viscosity,  $r$  and  $L$  the MT radius and length. The time evolution equation of the phase variable  $\phi(s, t)$  and elastic displacement  $\rho_{el}(s, t)$  is given by the coupled Langevin equations  $\frac{\delta E}{\delta \phi} = -\frac{\delta P_{diss}}{\delta \phi} + \Gamma_{\phi}$  and  $\frac{\delta E}{\delta \rho_{el}} = -\frac{\delta P_{diss}}{\delta \rho_{el}} + \Gamma_{\rho}$  with  $\Gamma_{\phi/\rho}$  the thermal noise term. In general this dynamics is highly non-linear however in the experimentally relevant regime where the behavior is dominated by the wobbling mode the equations simplify greatly and we end up with a simple diffusive behavior of the wobbling mode  $\frac{d}{dt}\phi_0(t) = \frac{1}{\xi_{tot}}L^{-1} \int_0^L \Gamma_{\phi}(s, t) ds$  with a friction constant given by  $\xi_{tot} = \xi_{int} + \xi_{ext}$  where  $\xi_{ext} = 2\xi_{\perp}\kappa_0^2q_0^{-4}((1 + \cos Lq_0) - 4 \sin Lq_0 + q_0^3L^3/3)$ . For comparison with the experiment we compute the time correlation of the  $y$  deflection. A short calculation gives  $\langle y_{pol}(L, t)y_{pol}(L, t') \rangle \propto e^{-|t-t'|/\tau(L)}$  with the relaxation time  $\tau(L) \approx L\xi_{tot}/k_B T$ . For small lengths,  $\tau(L) \approx L\xi_{int}/k_B T$  is dominated by internal dissipation while for large lengths  $\tau(L) \approx \frac{\xi_{\perp}}{3k_B T}(\kappa_0/q_0)^2 L^3$ . A careful analysis of the experimental data [5] reveals in fact the latter scaling. An independent single exponent fit gives  $\tau \propto L^{\alpha}$  with  $\alpha = 2.9$ . Using the value  $(\kappa_0/q_0)^2 \approx 4.8 \times 10^{-3}$  from Fig. 2 and  $\xi_{\perp} \approx 2\eta$  with  $\eta = 10^{-3} Pa \cdot s$  [23] we find the theoretical value  $\tau_{th}/L^3 = 7.9 \times 10^{14} s/m^3$  that can be compared with the fit of experimental data (Fig. 3)  $\tau_{fit}/L^3 = 6.25 \times 10^{14} s/m^3$ . The excellent agreement of both the exponent and the prefactor leads us again to the strong conclusion that in these experiments the clamped MT is an almost rigid helical polymorphic rotor whose behavior is dominated by the zero energy ("wobbling") mode and hydrodynamic dissipation. For very short MTs the linearly scaling internal dissipation dominates and we could measure  $\xi_{int}$  from the limit value of  $\tau_{th}/L$ , for  $L \rightarrow 0$ . For the available data  $L > 2 \mu m$  [5] this plateau-regime is not yet fully developed and we can only provide an upper estimate from the data  $\xi_{int} \lesssim 4 \times 10^{-17} Ns$ .

**Conclusion.** The MT fluctuations are well described - both dynamically and statically - by the bistable tubulin model and the reason for appearance of MT helices becomes obvious. The otherwise mysterious lateral fluctuations reflected in  $l_p^*(L) \sim L^1$  and  $\tau_p(L) \sim L^3$  scaling are mere consequences of the "wobbling motion" of a polymorphic cooperatively switching helical lattice. We speculate that the implied conformational multistability of tubulin and the allosteric interaction are not just nature's way to modulate the elastic properties of its most important cytoskeletal mechano-element. It could also be a missing piece in the puzzle of dynamic instability. Another intriguing possibility of using this switch for long range conformational signalling in vivo, could hardly have been overlooked by evolution. I.M.K thanks

Francesco Pampaloni for stimulating discussions.

\* Email: [kulic@unistra.fr](mailto:kulic@unistra.fr)

- [1] J. Howard, *Mechanics of Motor Proteins and the Cytoskeleton*, Sinauer Press 2001; L. A. Amos & Amos W. G., *Molecules of the Cytoskeleton*, Guilford Press 1991
- [2] I.M.Kulic et al. Proc. Natl. Acad. Sci. USA 105, 10011 (2008).
- [3] P. Venier et al. J. Biol. Chem. 269, 13353 (1994).
- [4] Pampaloni et al. Proc. Natl. Acad. Sci. USA. 103, 10248 (2006).
- [5] K.M. Taute et al, Phys. Rev. Lett. 100, 028102 (2008).
- [6] M. Janson & M. Dogterom, Biophys. J. 87, 2723 (2004); C. Brangwynne et al. Biophys. J. 93, 346 (2007).
- [7] M. Kurachi, M. Hoshi, & H. Tashiro. Cell Motil. Cytoskel. 30, 221 (1995); T. Takasone et al, Jpn. J. Appl. Phys. 41, 30153019 (2002); A. Kis, et al. Phys. Rev. Lett. 89, 248101 (2002); T. Kim et al. Biophys J. 94, 3880 (2008).
- [8] Keller et al. Biophys. J. 95, 1474 (2008).
- [9] C. Heussinger, M. Bathe & E. Frey, Phys. Rev. Lett. 99, 048101 (2007); H. Mohrbach & I.M. Kulic, Phys. Rev. Lett. 99, 218102 (2007).
- [10] We will focus on the simplest case of equilibrated, taxol stabilized MTs where dynamic instability is absent yet the very rich thermal behavior i-iii is pronounced.
- [11] S. Asakura, Advan. Biophys. (Japan) 1, 99 (1970); C. R. Calladine, Nature (London) 255, 121 (1975).
- [12] S. V. Srigiriraju & T. R. Powers Phys. Rev. Lett. 94, 248101 (2005); H. Wada and R. R. Netz, Europhys. Lett, 82, 28001 (2008)
- [13] C. Elie-Caille et al., Curr. Biol. 17, 17651770 (2007).
- [14] I.A.T. Schaap et al. Biophys. J. 91, 15211531 (2006).
- [15] L. A. Amos and W. B. Amos, J. Cell. Sci. Suppl. 14, 95101 (1991).
- [16]  $\varepsilon_{pol} = \varepsilon_{PF}\sigma_n(s) [I_{[R-2d_{PF}, R-d_{PF}]}(r) - I_{[R-d_{PF}, R]}(r)] \cdot I_{[\frac{2\pi}{N}n+q_0s, \frac{2\pi}{N}(n+1)+q_0s]}(\alpha)$  where  $I_{[.]}(x) = 1$  if  $x \in [.]$  and 0 otherwise,  $d_{PF}$  the PF diameter and  $q_0$  the natural lattice twist.
- [17] D. Chrétien et al, J. Cell. Bio. 117, 1031-1040 (1992); S.Ray, E.Meyhofer, R. A. Milligan, and J. Howard, J. Cell Biol., 121,1083, (1993).
- [18] Phase  $\phi$  fluctuations are induced by double defects which carry a limited local energy cost  $\Delta E = 2Jn$  ( $n$  being the number of double defects).  $|P|$  variations are induced by single defects having in general larger energy cost that grows with their end distance, cf. Fig.1d.
- [19] This mode has a  $N$  fold symmetry however for large number of PFs  $N = 11 - 15$  it can be approximated as continuous.
- [20] Another more common definition, from angular correlation  $\langle \cos(\theta(s) - \theta(s')) \rangle$  exhibiting a similarly rich behavior as  $l_p^*$  (yet a distinct functional form) will be discussed elsewhere.
- [21] In the plateau region the helix loses its "coherence" and the collective rigid rotational conical motion softens until an uncorrelated segment movement becomes dominant.
- [22] N. Kol et al. Nano Lett. 5, 1343 (2005).
- [23] In the experimental range [5] of  $2.2\mu m < L < 28\mu m$  :  $\xi_{\perp} \approx 1.6\eta - 2.3\eta$  is almost length independent.